March 15, 2017

SUPPORTING INFORMATION

A New Wavelet Denoising Method for Experimental Time Domain Signals: Pulsed Dipolar ESR

*Madhur Srivastava[1,2], Elka R. Georgieva[1,3†], and Jack H. Freed[1,3]**

[1]National Biomedical Center for Advanced ESR Technology, Cornell University, Ithaca, NY 14853, USA

[2]Meinig School of Biomedical Engineering, Cornell University, Ithaca, NY 14853, USA

[3]Department of Chemistry and Chemical Biology, Cornell University, Ithaca, NY 14853, USA

*Corresponding Author: jhf3@cornell.edu

† Current Institution: Weill Cornell Medical College, New York, NY 10065, USA

TABLE OF CONTENTS

S1. INTRODUCTION

We show in Fig. S1 the Detail and Approximation components of an experimental signal using wavelet "db6." In Fig. S2, the scaling and wavelet functions of the "db6" wavelet are shown, which are used to generate the Approximation and Detail components, respectively. We show in Figs. S3 to S8 comparisons of some of the WavPDS results from Figs. 4, 5, 7, and 8 with the standard methods noted below. These comparisons are also summarized in Tables S1 to S6. In all cases, WavPDS outperforms the other methods. In Fig. S9, we show an example of denoising before baseline subtraction and its utility in detecting baseline.

In Figs. S10 & S11, we show L-curve plots for determining λ both for noisy and denoised data. We distinguish between the $\lambda_{TIKR}^{L-Curve}$ obtained by locating the point of maximum curvature and those from manual adjustment λ_{TIKR}^{OPT} to best compare with the reference. Whereas they differ for the noisy signals, they are the same for the denoised signals. A comparison of WavPDS and a low-pass filter is shown in Fig. S12. In Fig. S13, the denoised echo signal is shown using this new method.

S2. DATA GENERATION METHODS

a. Model Signal (Figs. S3-S4): Bimodal

The model signal was generated from two Gaussian distributions centered at 4 nm and 5 nm with a standard deviation of 0.3 nm. The peak height of the first peak is 80% of the second peak. White Gaussian noise was added to generate the Noisy signals at SNR = 3 (Fig. S3A, **Red**) and SNR = 10 (Fig. S4A, **Red**).

b. Experimental Signal (Figs. S5-S6): Unimodal

The experimental signal was generated from T4 Lysozyme spin-labeled at mutant 44C/ 135C with 63 μM concentration (cf. Section 2.E for details). The signal acquisition time was 14 min (SNR = 3.8, cf. Fig. S5A, **Red**) and 112 min (SNR = 6.8, cf. Fig. S6A, **Red**).

c. Experimental Signal (Figs. S7-S8): Bimodal

The experimental signal was generated from T4 Lysozyme spin-labeled admixture of mutants 8C/44C and 44C/135C at concentrations of 44 μM and 47 μM, respectively (cf. Section 2.E for details). The signal acquisition time was 8 min (SNR = 11, cf. Fig. S7A, **Red**) and 48 min (SNR = 31, cf. Fig. S8A, **Red**).

S3. STANDARD WAVELET DENOISING METHODS

We compare our WavPDS method with the current standard wavelet denoising methods such as Minimax[1] and SUREShrink[2] for bimodal model signal (Figs. S3-S4) and unimodal and bimodal experimental signals (Figs. S5-S8) using the same Daubechises "db6" wavelet. They both are used to select optimal noise thresholds for the Detail components in the wavelet domain. Although there are many new wavelet denoising methods, these two methods are widely used and perform well for all types of signals. We compared our new method with these two methods and others in our previous paper.[3]

a. Noise Thresholding Function

Both hard and soft thresholding were used for Minimax and SUREShrink method to obtain denoised coefficients. They are referred as Minimax-Hard and SUREShrink-Hard for hard thresholding, and Minimax-Soft and SUREShrink-Soft for soft

thresholding in Figs. S3-S8. The hard (Eq. S1) and soft (Eq. S2) thresholding are defined as

$$D'_j[n] = \begin{cases} 0, for & |D_j[n]| < \lambda_j \\ D_j[n], & otherwise \end{cases} \quad \text{(S1)}$$

and

$$D'_j[n] = \begin{cases} 0, for & |D_j[n]| < \lambda_j \\ sgn\big(D_j[n]\big)\left(\big|D_j[n]\big| - \lambda_j\right), & otherwise \end{cases} \quad \text{(s2)}$$

where $D_j[n]$ and $D'_j[n]$ are the noisy and denoised Detail component, respectively, at the j^{th} Decomposition level, and λ_j is the noise threshold selected for the j^{th} Detail component using the Minimax or SUREShrink method.

b. Decomposition Level Selection

For Minimax and SUREShrink methods, the decomposition level that resulted in the denoised signal with highest SNR was selected. To calculate SNR, model data was used as a reference for model signals and WavPDS denoised data at 952 min (unimodal, Figs. S5-S6) and 360 min (bimodal, Figs. S5-S6) was used for experimental signals.

c. Signal Flipping

Like WavPDS, the signal $S(t)$ was flipped to $S(-t)$ (i.e., time reversed) before applying the standard denoising methods. This is to avoid distorting the initial ($t = 0$) signal as mentioned in Section 2.A. The flipped signal contains the same information as that of the non-flipped signal.

S4. DETAILS OF PLATFORM AND SOFTWARE

A machine with Intel Core i5-4590 CPU @ 3.30 GHz processor, Windows 7 operating system, 16 GB RAM, and 64-bit operating system was used as the platform. Denoising was performed using MATLAB 2014b. Built-in *wden* was used to denoise signals for the Minimax and SUREShrink wavelet denoising methods. WavPDS codes were written and implemented in MATLAB. Tikhonov Regularization (TIKR)[4] and Maximum Entropy Method (MEM)[5] codes written for MATLAB available on ACERT website (https://acert.cornell.edu/index_files/acert_resources.php) were used to generate $P(r)$. For WavPDS and standard methods, Daubechises 6 wavelet ("db6") was used for Discrete Wavelet Transform (DWT).

REFERENCES

(1) Donoho, D. L.; Johnstone, J. M. Ideal Spatial Adaptation by Wavelet Shrinkage. *Biometrika* **1994**, *81* (3), 425–455.

(2) Donoho, D. L.; Johnstone, I. M. Adapting to Unknown Smoothness via Wavelet Shrinkage. *J. Am. Stat. Assoc.* **1995**, *90* (432), 1200.

(3) Srivastava, M.; Anderson, C. L.; Freed, J. H. A New Wavelet Denoising Method for Selecting Decomposition Levels and Noise Thresholds. *IEEE Access* **2016**, *4*, 3862–3877.

(4) Chiang, Y.-W.; Borbat, P. P.; Freed, J. H. The Determination of Pair Distance Distributions by Pulsed ESR Using Tikhonov Regularization. *J. Magn. Reson.* **2005**, *172* (2), 279–295.

(5) Chiang, Y.-W.; Borbat, P. P.; Freed, J. H. Maximum Entropy: A Complement to Tikhonov Regularization for Determination of Pair Distance Distributions by Pulsed ESR. *J. Magn. Reson.* **2005**, *177* (2), 184–196.

(6) Borbat, P. P.; Freed, J. H. Multiple-Quantum ESR and Distance Measurements. *Chem. Phys. Lett.* **1999**, *313* (1–2), 145–154.

(7) Sil, D.; Lee, J. B.; Luo, D.; Holowka, D.; Baird, B. Trivalent Ligands with Rigid DNA Spacers Reveal Structural Requirements for IgE Receptor Signaling in RBL Mast Cells. *ACS Chem. Biol.* **2007**, *2* (10), 674–684.

S5. WAVELET COMPONENTS OF AN EXPERIMENTAL PDS SIGNAL

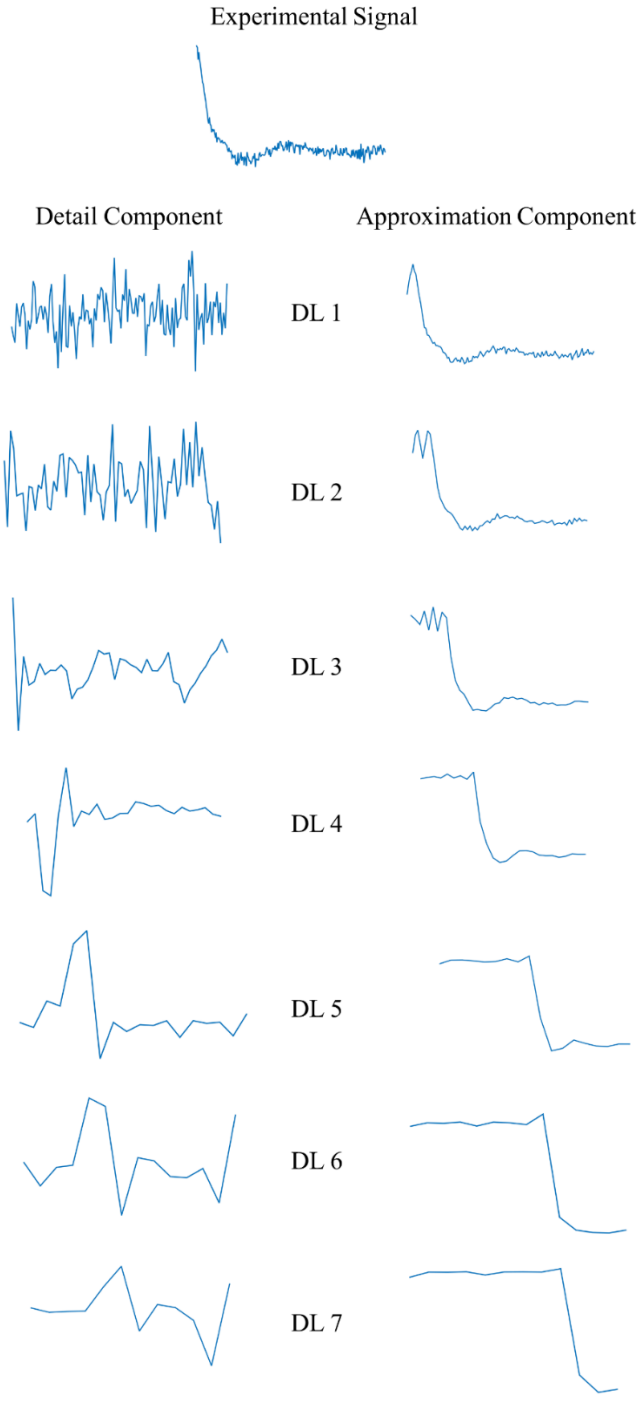

Fig. S1: The Detail and Approximation components of a PDS signal. DL is the decomposition level.

S6. SCALING AND WAVELET FUNCTIONS OF THE "db6" WAVELET

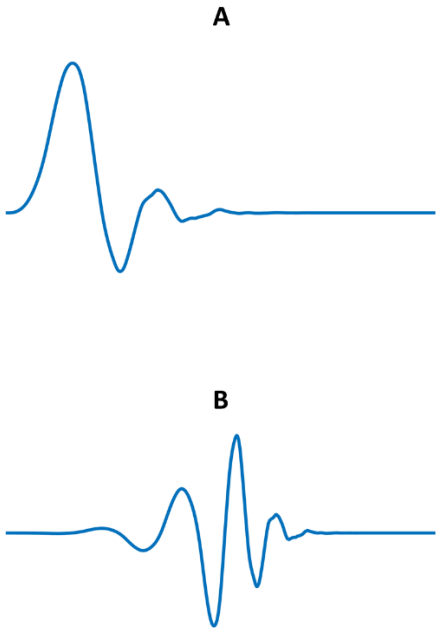

Fig. S2: The "db6" wavelet used. A) The Scaling function is used to generate Approximation components (see Eq. 11); B) The Wavelet function is used to generate Detail components (see Eqs. 8 and 9).

S7. COMPARISON OF STANDARD METHODS WITH WavPDS

Table S1: Comparison of WavPDS and Standard Denoising methods (Minimax and SUREShrink) on Noisy signal for Model Data - Bimodal Distribution at SNR 3 (cf. Fig. S3).

Method	**SNR**	χ^2	**SSIM**	λ_{TIKR}^{OPT}	$\lambda_{TIKR}^{L-Curve}$
Noisy	3	0.333	0.008	60	904
Minimax-Hard	6	0.167	0.282	40	897
Minimax-Soft	19	0.053	0.626	30	76
SUREShrink-Hard	6	0.179	0.119	30	872
SUREShrink-Soft	9	0.107	0.226	30	99
New Method	378	0.0026	0.945	10	10

Table S2: Comparison of WavPDS and Standard Denoising methods (Minimax and SUREShrink) on Noisy signal for Model Data - Bimodal Distribution at SNR 10 (cf. Fig. S4).

Method	**SNR**	χ^2	**SSIM**	λ_{TIKR}^{OPT}	$\lambda_{TIKR}^{L-Curve}$
Noisy	10	0.100	0.107	20	85
Minimax-Hard	18	0.054	0.607	15	79
Minimax-Soft	50	0.020	0.871	15	39
SUREShrink-Hard	18	0.054	0.572	15	77
SUREShrink-Soft	38	0.026	0.775	15	51
New Method	1850	0.0005	0.953	3	3

Table S3: Comparison of WavPDS and Standard Denoising methods (Minimax and SUREShrink) on Noisy signal for Experimental Data - Unimodal Distribution at signal acquisition time 14 min (SNR 3.8; cf. Fig. S5).

Method	**SNR**	χ^2	**SSIM**	λ_{TIKR}^{OPT}	$\lambda_{TIKR}^{L-Curve}$
Noisy	3.8	0.263	0.038	30	0.08
Minimax-Hard	6	0.160	0.386	10	28
Minimax-Soft	13	0.079	0.306	10	4
SUREShrink-Hard	7	0.142	0.288	10	24
SUREShrink-Soft	11	0.094	0.313	10	26
New Method	488	0.0021	0.967	0.08	0.08

Table S4: Comparison of WavPDS and Standard Denoising methods (Minimax and SUREShrink) on Noisy signal for Experimental Data - Unimodal Distribution at signal acquisition time 112 min (SNR 6.8; cf. Fig. S6).

Method	**SNR**	χ^2	**SSIM**	λ_{TIKR}^{OPT}	$\lambda_{TIKR}^{L-Curve}$
Noisy	6.8	0.190	0.135	8	25
Minimax-Hard	12	0.085	0.364	5	0.07
Minimax-Soft	23	0.043	0.486	5	3
SUREShrink-Hard	10	0.098	0.177	5	0.08
SUREShrink-Soft	17	0.058	0.442	5	4
New Method	909	0.0011	0.995	0.07	0.07

Table S5: Comparison of WavPDS and Standard Denoising methods (Minimax and SUREShrink) on Noisy signal for Experimental Data - Bimodal Distribution at signal acquisition time 8 min (SNR 11; cf. Fig. S7).

Method	**SNR**	χ^2	**SSIM**	λ_{TIKR}^{OPT}	$\lambda_{TIKR}^{L-Curve}$
Noisy	11	0.086	0.156	10	255
Minimax-Hard	19	0.052	0.418	8	46
Minimax-Soft	33	0.030	0.708	8	31
SUREShrink-Hard	15	0.065	0.266	8	119
SUREShrink-Soft	23	0.044	0.469	8	40
New Method	1046	0.0009	0.961	0.09	0.09

Table S6: Comparison of WavPDS and Standard Denoising methods (Minimax and SUREShrink) on Noisy signal for Experimental Data - Bimodal Distribution at signal acquisition time 48 min (SNR 31; cf. Fig. S8).

Method	**SNR**	χ^2	**SSIM**	λ_{TIKR}^{OPT}	$\lambda_{TIKR}^{L-Curve}$
Noisy	31	0.032	0.573	5	118
Minimax-Hard	49	0.021	0.798	1	3
Minimax-Soft	89	0.011	0.956	5	0.78
SUREShrink-Hard	44	0.023	0.772	3	45
SUREShrink-Soft	84	0.012	0.930	2.26	2
New Method	3333	0.0003	0.999	0.08	0.08

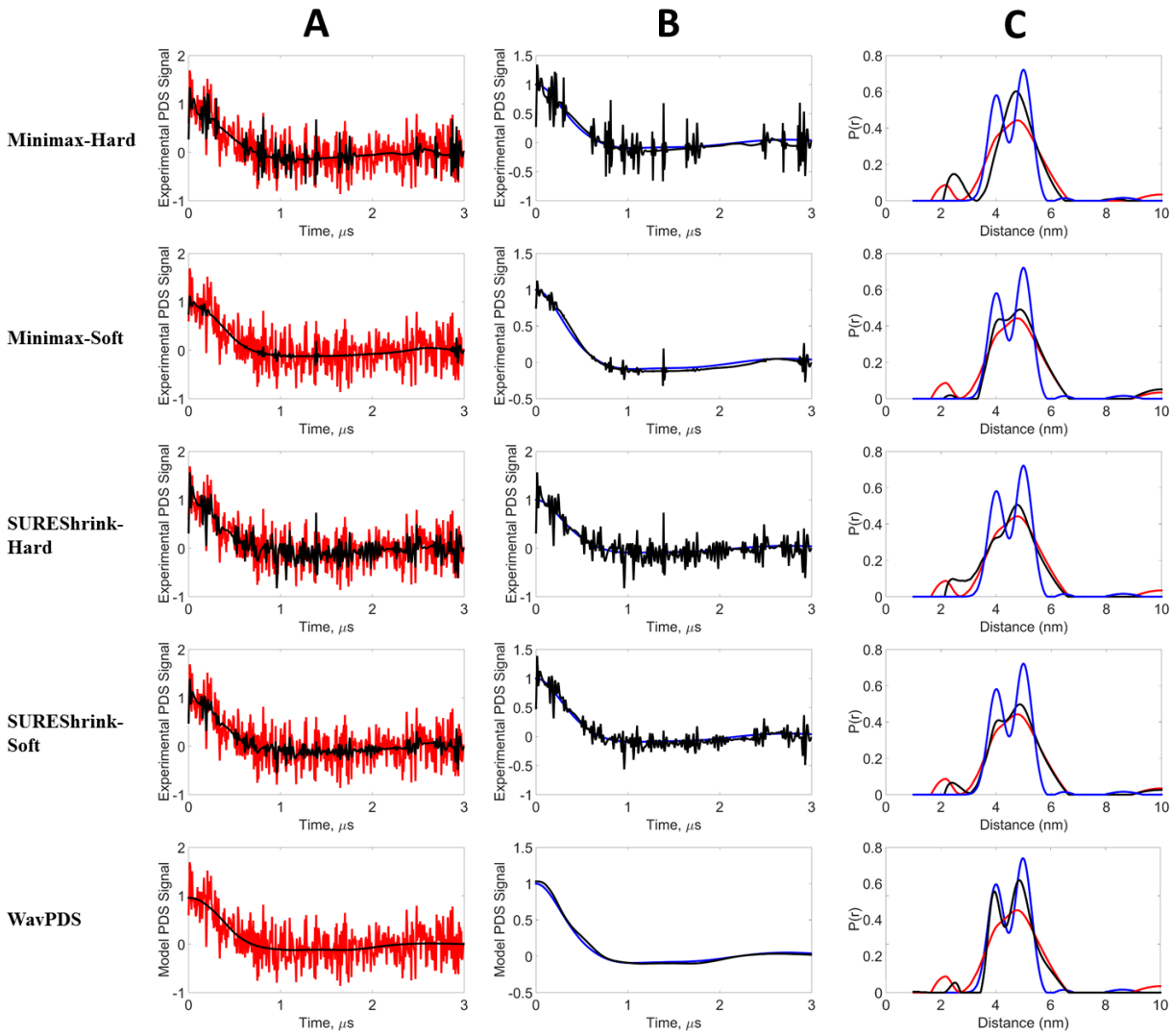

Figure S3: Model Data - Bimodal Distribution (cf. Fig. 5) with SNR = 3: Results of new WavPDS method compared to standard wavelet denoising methods such as Minimax and SUREShrink using hard and soft noise thresholding. **Blue** – Model Signal (Reference), **Red –** Noisy Signal, **Black** – Denoised Signal. **A)** Comparison of Noisy and Denoised signals; **B)** Comparison of Model signals and Denoised signals; **C)** Distance Distributions from Noisy, Denoised, and Model signals.

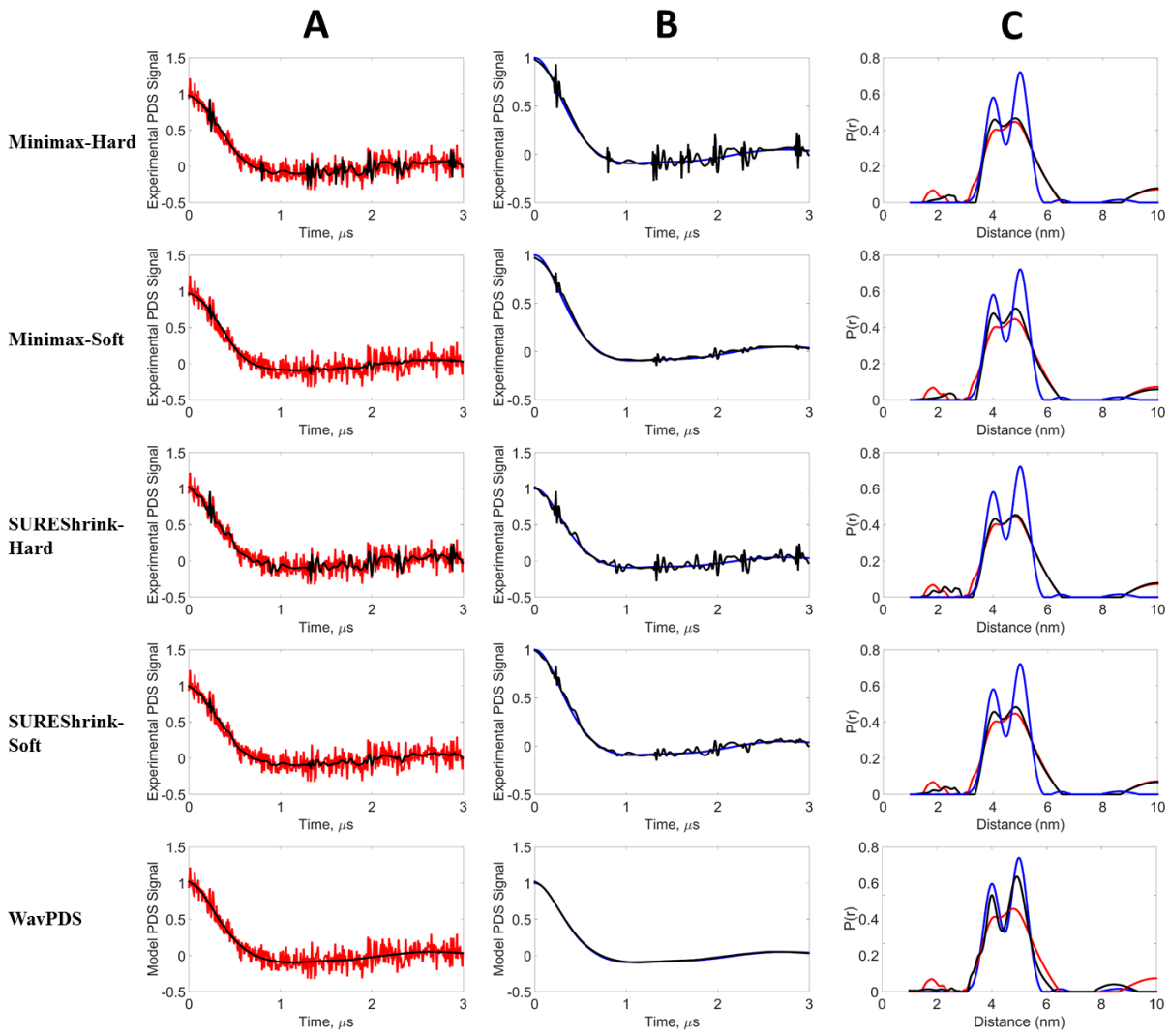

Figure S4: Model Data - Bimodal Distribution (cf. Fig. 5) with SNR = 10: Results of new WavPDS method compared to standard wavelet denoising methods such as Minimax and SUREShrink using hard and soft noise thresholding. **Blue** – Model Signal (Reference), **Red** – Noisy Signal, **Black** – Denoised Signal. **A)** Comparison of Noisy and Denoised signals; **B)** Comparison of Model signals and Denoised signals; **C)** Distance Distributions from Noisy, Denoised, and Model signals.

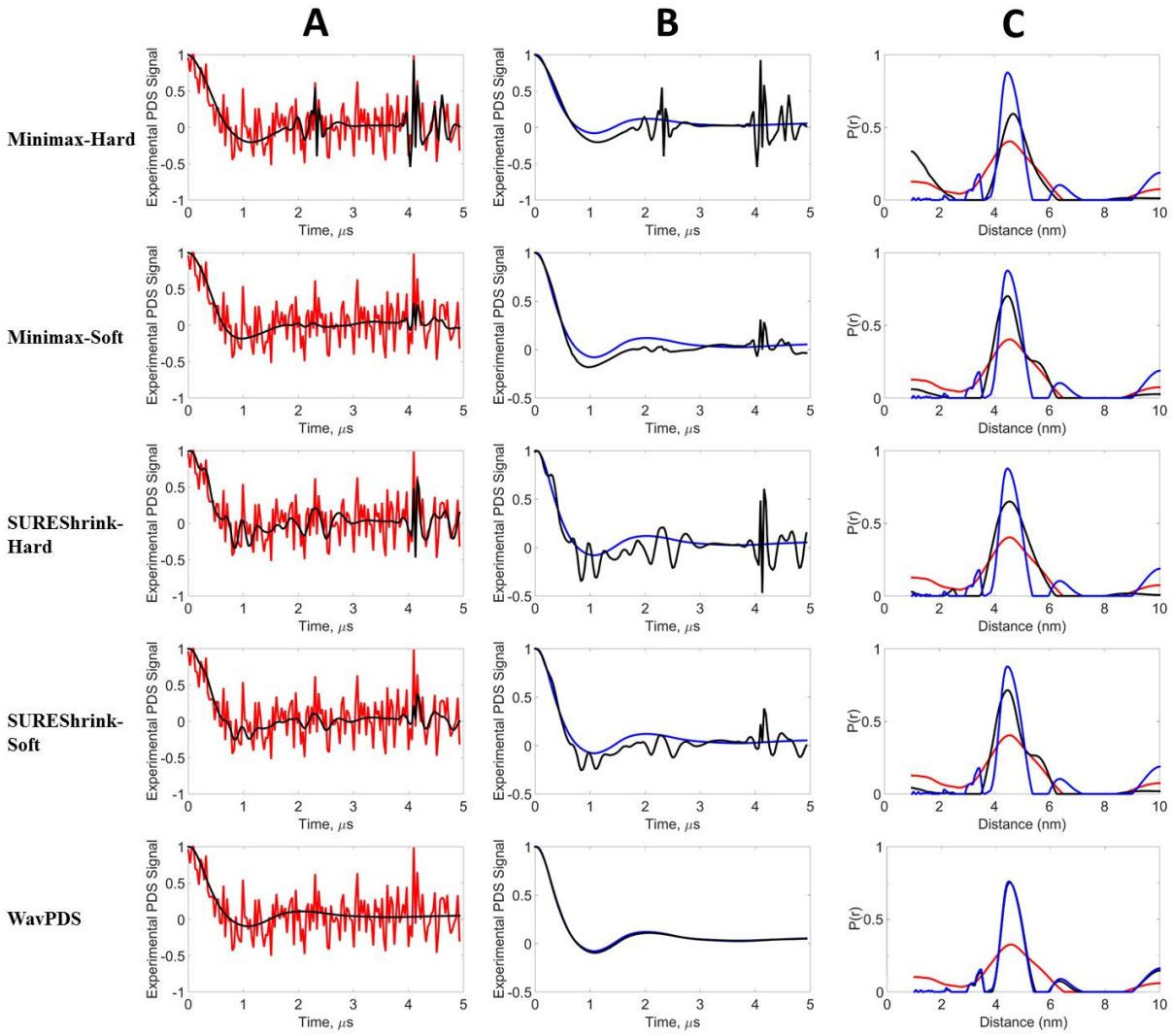

Figure S5: Experimental Data - Unimodal Distribution (cf. Fig. 7) with 14 min of acquisition time (SNR = 3.8): Results of WavPDS method compared to standard wavelet denoising methods such as Minimax and SUREShrink using hard and soft noise thresholding. **Blue** – Model Signal (Reference), **Red** – Noisy Signal, **Black** – Denoised Signal. **A)** Comparison of Noisy and Denoised signals; **B)** Comparison of Reference signals and Denoised signals; **C)** Distance Distributions from Noisy, Denoised, and Reference signals. Denoised signal at 952 min was used as the Reference.

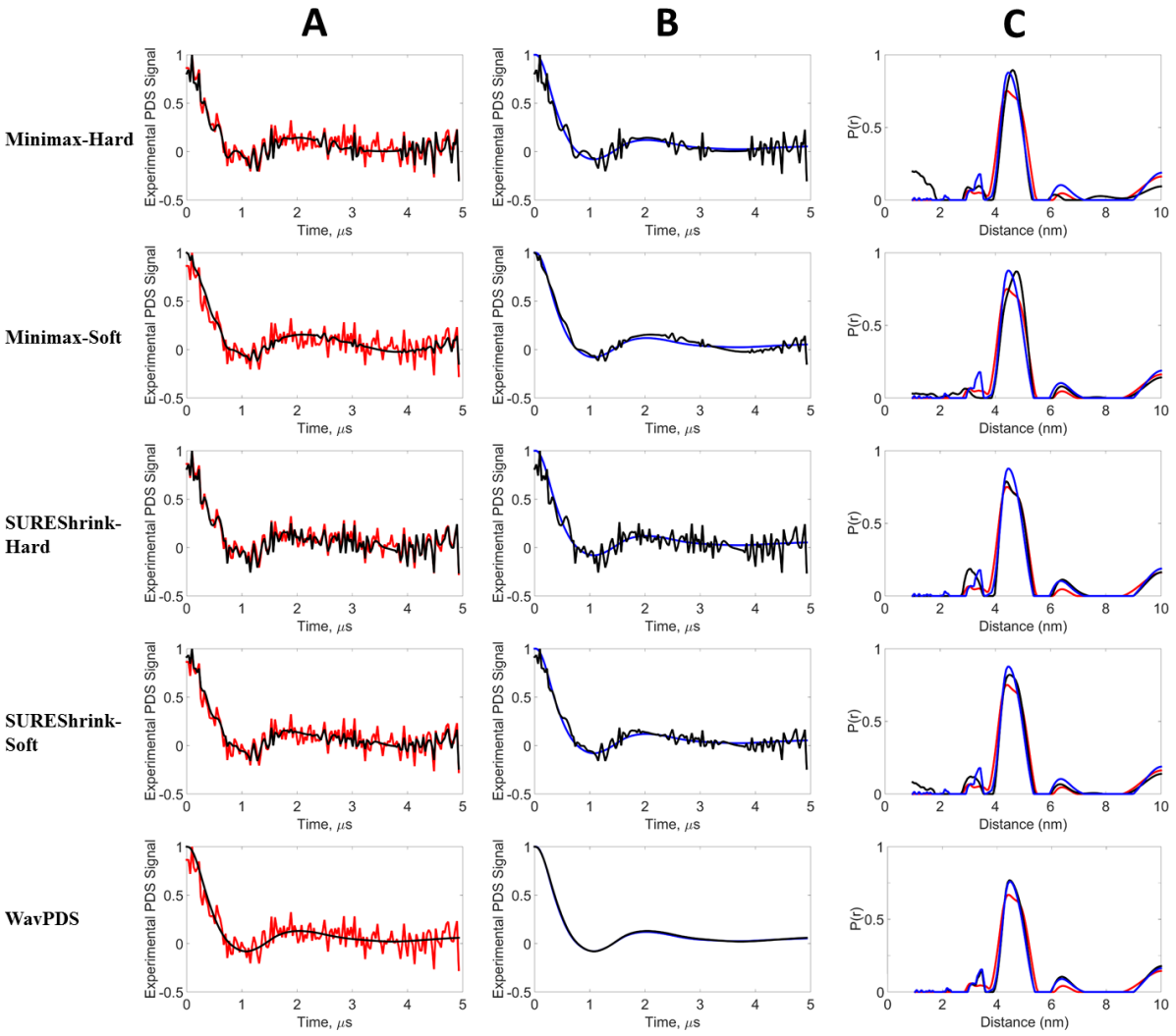

Figure S6: Experimental Data - Unimodal Distribution (cf. Fig. 7) with 112 min of acquisition time (SNR = 6.8): Results of new WavPDS method compared to standard wavelet denoising methods such as Minimax and SUREShrink using hard and soft noise thresholding. **Blue** – Reference Signal, **Red** – Noisy Signal, **Black** – Denoised Signal. **A)** Comparison of Noisy and Denoised signals; **B)** Comparison of Reference signals and Denoised signals; **C)** Distance Distributions from Noisy, Denoised, and Reference signals. Denoised signal at 952 min was used as the Reference.

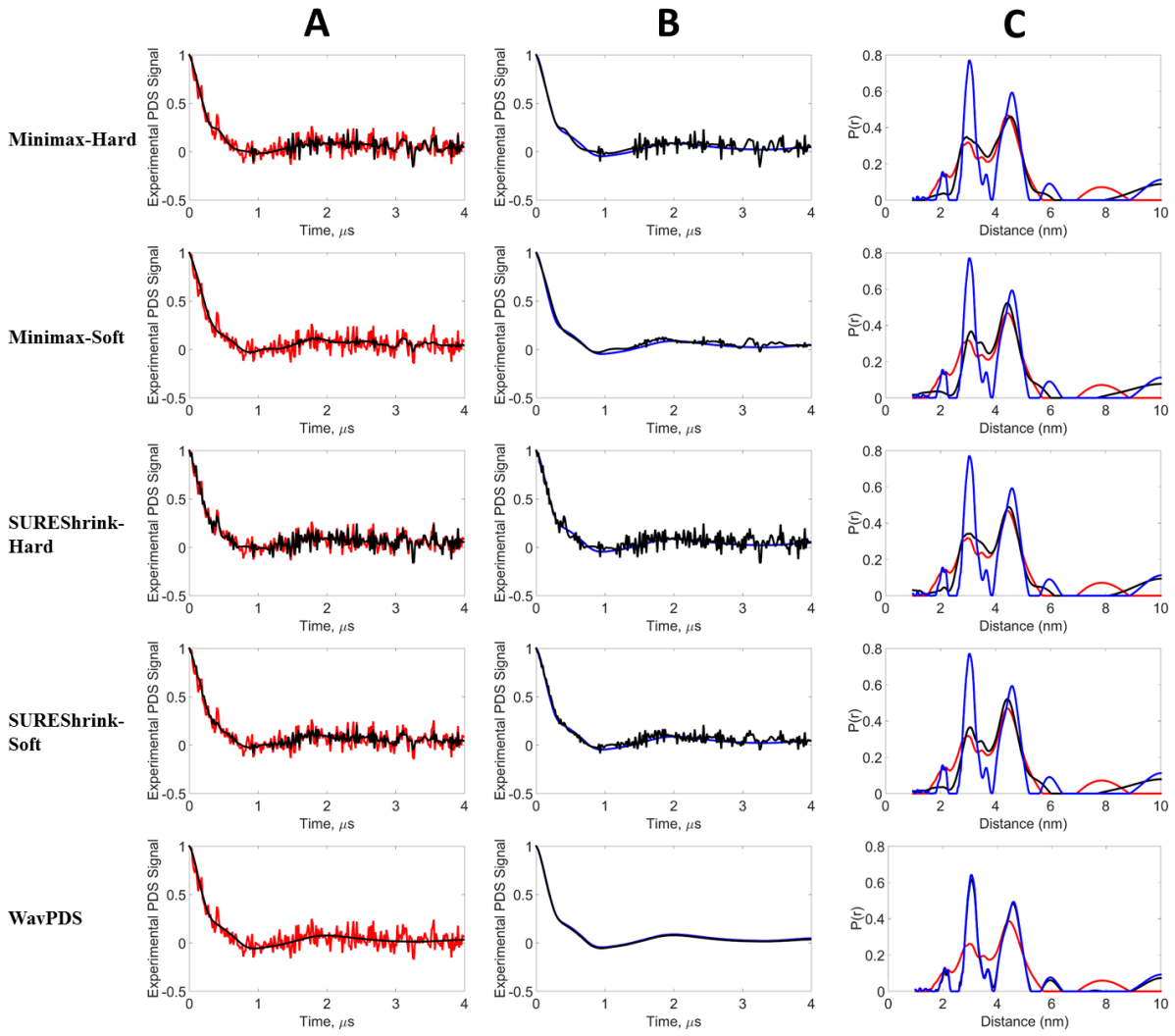

Figure S7: Experimental Data - Bimodal Distribution (cf. Fig. 8) with 8 min of acquisition time (SNR = 11): Results of new WavPDS method compared to standard wavelet denoising methods such as Minimax and SUREShrink using hard and soft noise thresholding. **Blue** – Reference Signal, **Red** – Noisy Signal, **Black** – Denoised Signal. **A)** Comparison of Noisy and Denoised signals; **B)** Comparison of Reference signals and Denoised signals; **C)** Distance Distributions from Noisy, Denoised, and Reference signals. Denoised signal at 360 min was used as the Reference.

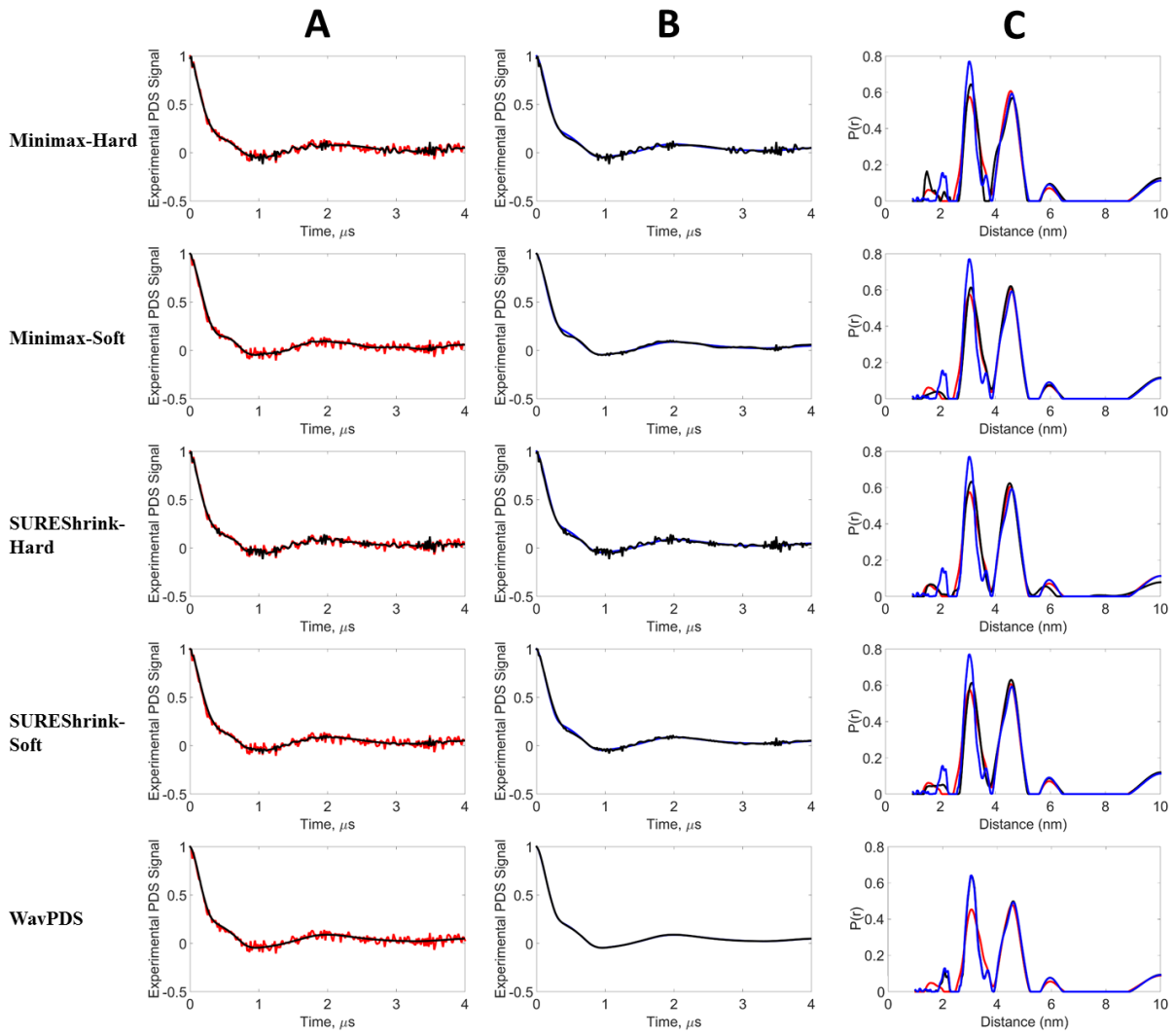

Figure S8: Experimental Data - Bimodal Distribution (cf. Fig. 8) with 48 min of acquisition time (SNR = 31): Results of new WavPDS method compared to standard wavelet denoising methods such as Minimax and SUREShrink using hard and soft noise thresholding. **Blue** – Reference Signal, **Red –** Noisy Signal, **Black** – Denoised Signal. **A)** Comparison of Noisy and Denoised signals; **B)** Comparison of Reference signals and Denoised signals; **C)** Distance Distributions from Noisy, Denoised, and Reference signals. Denoised signal at 360 min was used as the Reference.

S8. EXAMPLE OF SIGNAL DENOISING BEFORE BASELINE SUBTRACTION

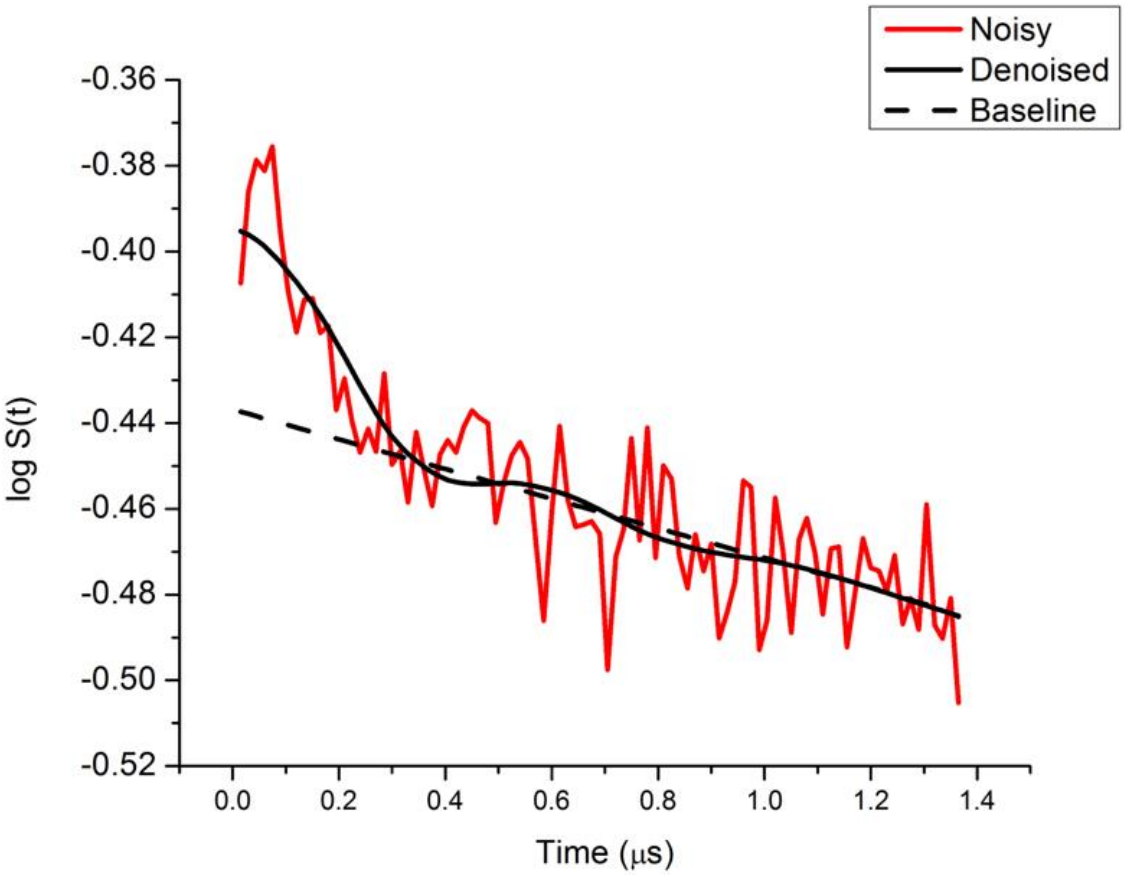

Figure S9: Comparison of Noisy signal (after 18 hr of signal averaging) and WavPDS Denoised signal before baseline subtraction. Baseline is determined by fitting the last several points of the denoised spectrum by a straight line. The *log* of the pulsed dipolar signal ($\log(S(t))$) is plotted versus the evolution time (μs) for a sub-μM concentration of spin labeled IgE cross-linked with trivalent DNA-DNP ligand in PBS buffer solution.[7] (After baseline removal the SNR is 3.8.) This figure was provided by Siddarth Chandrasekaran (ACERT).

S9. USE OF L-CURVE TO DETERMINE λ

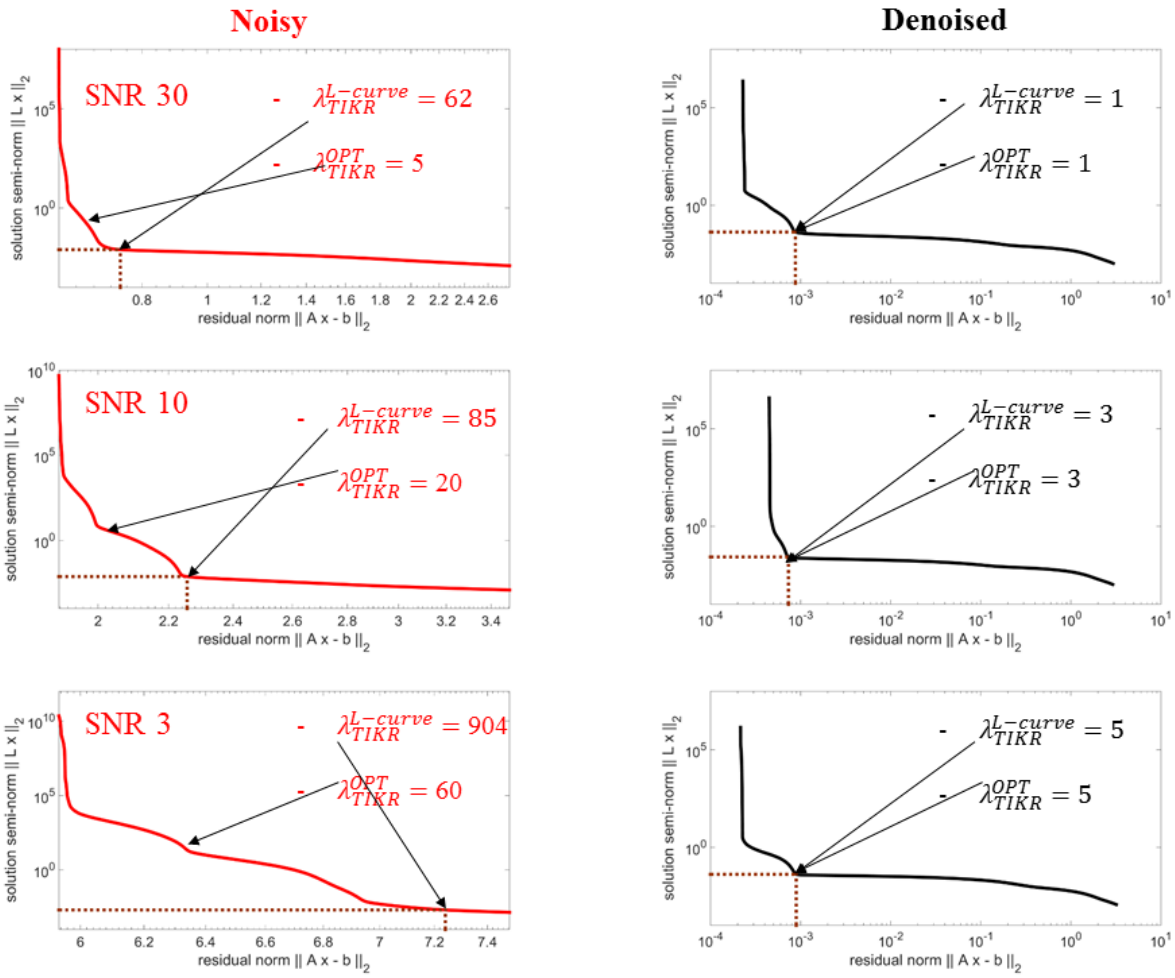

Figure S10: L-curve plots to determine λ for Noisy signals at SNRs 30, 10, and 3, and L-curve plots of their respective WavPDS Denoised signals for Model Data - Bimodal Distribution (as shown in Fig. 5). **Red** – Noisy Signal L-curve plots, **Black** – Denoised L-curve plots.

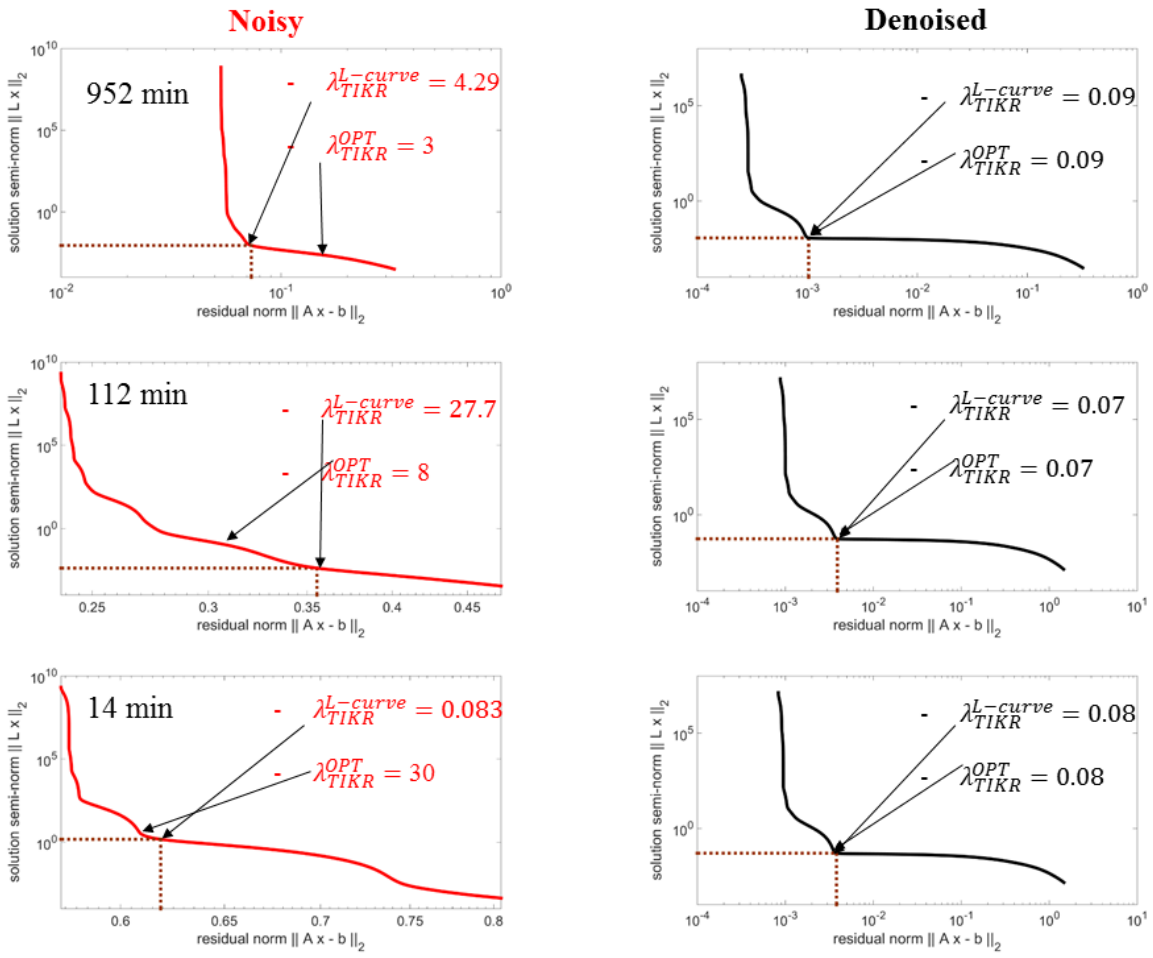

Figure S11: L-curve plot to determine λ for Noisy signal at signal acquisition times 952, 112, and 14 min, and the L-curve plot of their respective WavPDS Denoised signals for Experimental Data - Unimodal Distribution (cf. Fig. 7). **Red** –Noisy Signal L-curve plots, **Black** – Denoised L-curve plots.

S10. COMPARISON OF A LOW-PASS FILTER WITH WavPDS

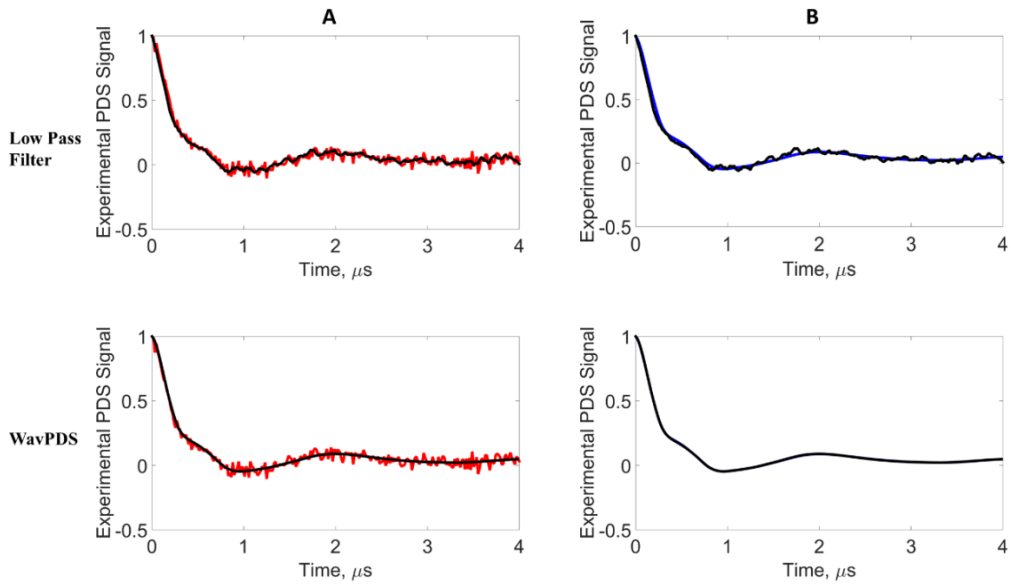

Fig. S12: Experimental Data—Bimodal Distribution (cf. Fig. 8) with 48 min of acquisition time (SNR = 31): Results of WavPDS method compared to low-pass filtering. **Blue**—Reference signal; **Red**—Noisy signal; **Black**—Denoised signal. A) Comparison of the Noisy and Denoised Signals; B) Comparison of Reference and Denoised signals. Denoised signal at 360 min was used as the Reference.

S11. EXAMPLE OF SPIN ECHO DENOISING

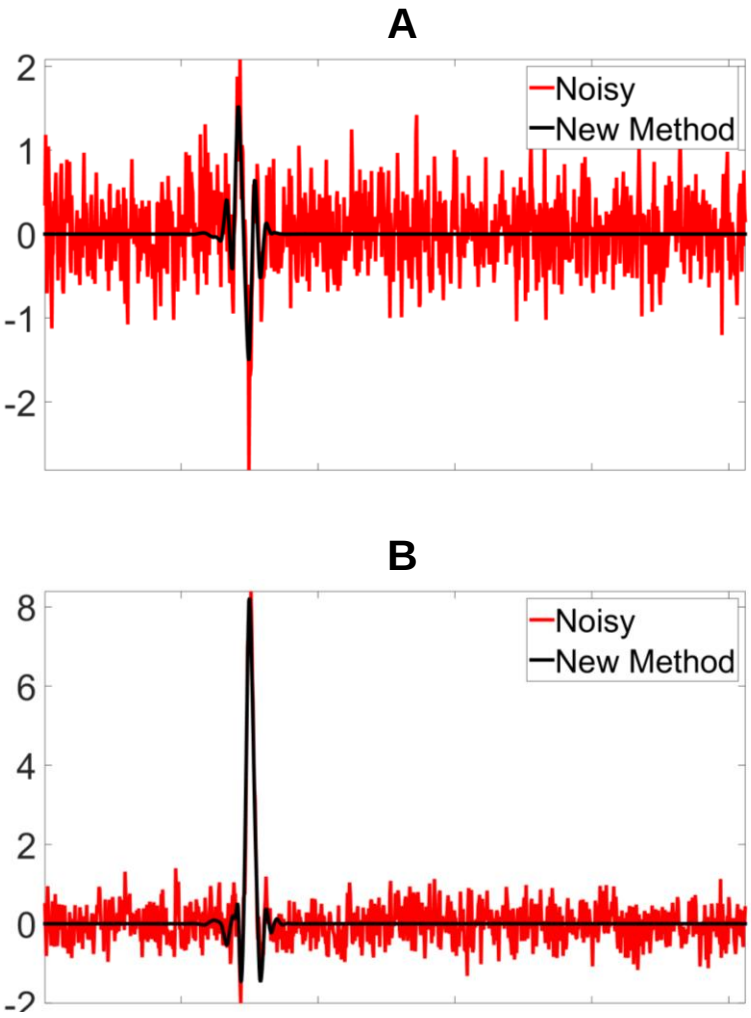

Figure S13: Echo Signal Denoising: **Red** - Original Noisy Signal, **Black** - Denoised Signal: **A)** Dispersion where SNR goes from 4 to 1.7×10^7 by denoising; **B)** Absorption where SNR of 19 becomes 9.0×10^6. The sample was a 20 μM solution of biradical $piperidinyl - CO_2 - (phenyl)_4 - O_2C - piperidinyl$ [6] and the $^{\pi}/_2$ and $^{\pi}/_2$ pulses were 2 ns providing full coverage. Coiflet 3 wavelet was used. This figure was provided by Dr. Peter Borbat (ACERT).